The Journal of Chemical Physics ARTICLE scitation.org/journal/jcp

Non-statistical fragmentation in photo-activated flavin mononucleotide anions

Cite as: J. Chem. Phys. 155, 044305 (2021); doi: 10.1063/5.0056415
Submitted: 10 May 2021 • Accepted: 7 July 2021 •
Published Online: 26 July 2021

Linda Giacomozzi,[1] Christina Kjær,[2] Steen Brøndsted Nielsen,[2] Eleanor K. Ashworth,[3] James N. Bull,[3] and Mark H. Stockett[1,a)]

AFFILIATIONS

[1] Department of Physics, Stockholm University, Stockholm, Sweden
[2] Department of Physics and Astronomy, Aarhus University, Aarhus, Denmark
[3] School of Chemistry, University of East Anglia, Norwich Research Park, Norwich, United Kingdom

[a)] **Author to whom correspondence should be addressed:** mark.stockett@fysik.su.se

ABSTRACT

The spectroscopy and photo-induced dissociation of flavin mononucleotide anions *in vacuo* are investigated over the 300–500 nm wavelength range. Comparison of the dependence of fragment ion yields as a function of deposited photon energy with calculated dissociation energies and collision-induced dissociation measurements performed under single-collision conditions suggests that a substantial fraction of photo-activated ions decompose through non-statistical fragmentation pathways. Among these pathways is the dominant photo-induced fragmentation channel, the loss of a fragment identified as formylmethylflavin. The fragment ion specific action spectra reveal electronic transition energies close to those for flavins in solution and previously published gas-phase measurements, although the photo-fragment yield upon excitation of the $S_2 \leftarrow S_0$ transition appears to be suppressed.

I. INTRODUCTION

Flavins are a common class of redox-active cofactors which catalyze a wide range of biochemical reactions, including metabolism.[1–3] The flavin mononucleotide (FMN, Fig. 1) and flavin adenine dinucleotide (FAD) forms are also well-known blue light sensors in enzymes and proteins that regulate DNA repair,[1] phototropism and circadian rhythms in plants,[4] and the perception of magnetic fields by some migratory birds.[5,6]

An important property of flavin cofactors facilitating their versatility in biology is tunability of the chromophore's electronic structure through the micro-environment of a host protein's chromophore binding pocket.[7,8] This micro-environment can have important consequences for the functioning of a flavoprotein, particularly for flavins that rely on photo-activation.[9] It is known that cellular redox equilibria can favor a particular resting redox state of a given flavoprotein,[10] leading to distinct absorption spectra. Furthermore, even for a given redox state, significant differences in the absorption spectra and associated excited state lifetimes of flavoprotein chromophores have been observed.[7] In order to *quantitatively* understand micro-environmental influences, the intrinsic absorption spectra of isolated chromophores are needed as a baseline reference.

Free flavins, i.e., those not bound in proteins, are ubiquitous in nature and are implicated as photo-sensitizers of reactions leading to the formation of cancer-causing singlet oxygen in the skin.[11] Photo-sensitized reactions involving flavins as well as photo-induced degradation of flavins themselves contribute to the tainting of many foods, particularly milk,[12] non-dairy milk alternatives,[13] and beer.[14] The photolysis of flavins in condensed phases is complex, with several competing intramolecular and intermolecular pathways.[15–24] Gas-phase photochemical experiments can help clarify this situation by revealing the intrinsic degradation channels which do not depend on solvent or biochemical environments.

The intrinsic absorption spectra and photo-degradation pathways of isolated macro-ions, such as flavins, can be investigated using gas-phase action spectroscopy techniques,[25] potentially revealing wavelength-dependent branching ratios for competing processes.[26] In the gas phase, individual perturbations to a molecule's electronic structure can be probed directly by preparing model nano-scale complexes containing a chromophore with other coupled chromophores,[27] one or a few solvent molecules,[28] protein

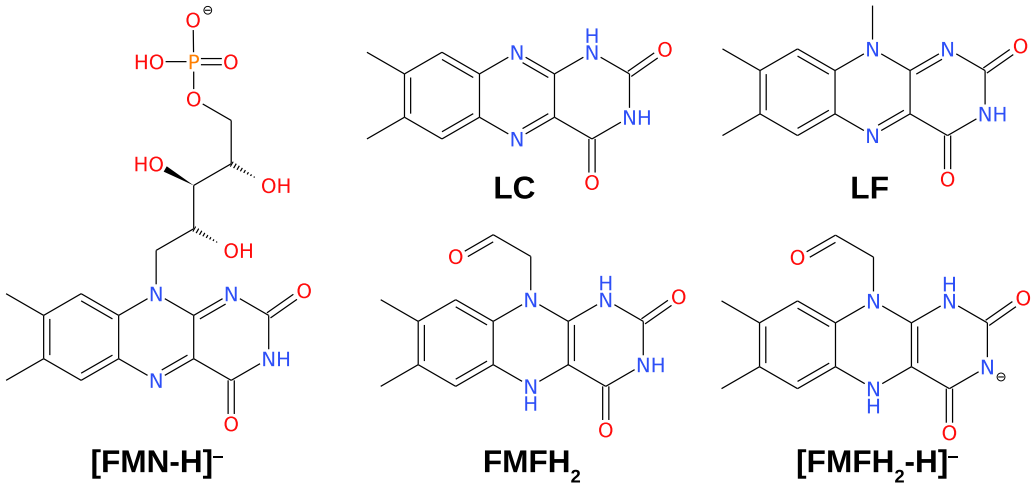

FIG. 1. Structures of deprotonated flavin mononucleotide ([FMN–H]$^-$), lumichrome (LC), lumiflavin (LF), formylmethylflavin ($FMFH_2$), and deprotonated formylmethylflavin ($[FMFH_2]^-$).

residues,[29] or other interaction partners that may be found at the protein interface.[30] Action and mass spectra of gas-phase ions are often directly comparable to state-of-the-art quantum chemical calculations, which are most frequently executed for isolated molecules or greatly simplified nano-environments.[31]

Action spectroscopy experiments can also guide complex molecular dynamics calculations by identifying the most important photochemical reaction pathways,[32,33] focusing an otherwise expensive exploration of the potential energy hypersurface. In the context of molecular fragmentation, statistical processes are those whose propensities can be calculated through statistical theories such as Rice–Ramsperger–Kassel–Marcus (RRKM), detailed balance, or phase space.[34,35] In a statistical fragmentation pattern, the relative product yields are weighted by Boltzmann factors, which depend exponentially on the dissociation energies, considering only reactions occurring on the electronic ground state after the activation energy has been statistically redistributed across all internal degrees of freedom. For photoactivated ions, statistical mechanisms imply that internal conversion to the ground electronic state occurs before dissociation. In contrast, non-statistical (sometimes called non-ergodic) fragmentation channels may be identified when the yield of a fragment exceeds that expected from statistical rate theories. Non-statistical pathways are often specific to the method of activation, in our case photoexcitation. However, it should be noted that the fragmentation processes for molecules such as flavins may have several competitive non-statistical and statistical pathways, leading to complex results; such situations are challenging to model with theory. In the present work, we show a propensity for non-statistical fragmentation channels in deprotonated flavin mononucleotide anions by comparing the mass spectra following activation by photons and collisions, as well as calculated dissociation energies.

Several groups have recently applied action spectroscopy to various members of the flavin family,[36] with numerous reports investigating the site-dependent influence of protonation or metalation on their electronic[37–41] and vibrational spectra.[42–44] Somewhat less attention has been paid to the photo-degradation of gaseous flavins, and nearly all such studies have focused on small sub-units such as lumichrome,[45,46] which lack the (phospho)ribityl sidechain present in many naturally occurring flavins. Recent studies by some of the present authors have suggested that photo-initiated proton transfer both to[47] and from[48] this sidechain are active photochemical pathways *in vacuo*.

Here, we report the first detailed study of the intrinsic absorption and photo-induced degradation of deprotonated flavin mononucleotide anions ([FMN–H]$^-$, Fig. 1). In this charge state, the dominant site of deprotonation is on the phosphoric acid group, which has a pK_a of around 2,[49] leaving the isoalloxazine chromophore ($pK_a \approx 10$)[50,51] in the neutral, fully oxidized form most common for flavins at physiological pH. Several of the present authors performed a photoisomerization action (PISA) spectroscopy study of [FMN–H]$^-$,[47] revealing facile structural rearrangement from the phosphate deprotomer to a ring deprotomer upon photoexcitation over the S_1 absorption band. The dominant electrosprayed form was shown to be deprotonated on the phosphate group. No fragmentation was observed in that experiment, presumably because the high buffer gas pressure (≈6 Torr) suppressed ground state dissociation processes. We are aware of two other studies in which FMN has been investigated using photo-induced dissociation (PID) mass spectrometry.[52,53] Both of these reports focused on protonated FMN. Guyon *et al.*[52] also provided a PID mass spectrum of [FMN–H]$^-$, but only for $m/z > 200$ and only at a single wavelength of 405 nm, which is shorter than the lowest singlet transition, complicating the interpretation. Intriguingly, the main PID fragments for protonated FMN are consistent with single bond cleavages along the ribityl tail. In contrast, the PID fragmentation pathways for [FMN–H]$^-$ involve more complex intramolecular rearrangements. Another important outcome from the study of Guyon *et al.* was application of a two-color femtosecond scheme (405 nm pump and 810 nm probe) with protonated FMN to

illustrate the variation of the branching ratio between the lumichrome and lumiflavin molecules produced by photofragmentation; no changes in the relative branching ratio were observed if the probe was delayed relative to the pump by up to 100 ps. The change in the branching ratio between lumichrome and lumiflavin was attributed to $S_n \leftarrow S_1$ excitations by the probe laser and implies that the excited state pumped at 405 nm lives for substantially longer than 100 ps. Whatever may be the detailed dynamics, the study provided compelling evidence for non-statistical photodissociation processes in some protonation states of FMN.

In the present paper, we report PID mass spectra for $[FMN–H]^-$ over a wider mass range, revealing further photochemical pathways and more definitive evidence for non-statistical photodissociation processes. In an additional set of experiments, we report the PID mass spectrum and action spectrum of $[FMN–H]^-$ complexed with betaine (trimethylglycine) zwitterions. The Zwitter-Ion Tagging Action (ZITA) spectroscopy technique was developed to identify electronic transitions with intramolecular charge transfer character[30,54–56] and is used in this work to probe the nature of the $S_1 \leftarrow S_0$ and $S_2 \leftarrow S_0$ transitions in $[FMN–H]^-$.

II. EXPERIMENTAL AND COMPUTATIONAL METHODS

A. Photo-induced dissociation

Photo-Induced Dissociation (PID) experiments were performed using the SepI accelerator mass spectrometer at Aarhus University.[57,58] Flavin mononucleotide sodium salt was purchased from Sigma-Aldrich and dissolved in methanol. Ions were transferred into the gas phase via electrospray ionization and stored in an octopole ion trap, which was emptied every 25 ms (40 Hz repetition rate). Ion bunches extracted from the octopole trap were accelerated to kinetic energies of 50 keV and the ions of interest (m/z = 455) were selected using a bending magnet. A high-intensity ns-pulsed optical parametric oscillator (OPO) laser system (EKSPLA NT342B) operating at a 20 Hz repetition rate was used to excite every second ion bunch. A home-built sum frequency generation unit combining the OPO signal (420–709 nm) with the 1064 nm pump generated light in the 304–420 nm range.[59] During the ≈5 ns irradiation time, the $[FMN–H]^-$ molecules had the possibility of absorbing multiple photons sequentially, i.e., returning to their electronic ground state in between each photon absorption. The laser beam was unfocused and the laser pulse energy was far below the regime where concerted multi-photon absorption (i.e., absorption by ions in electronically excited states) could occur. Fragment ions were separated using an electrostatic energy analyzer positioned after the laser–ion interaction region and counted with a channeltron detector. The difference in counts between the "laser-on" and "laser-off" injections is the photo-induced signal. The SepI instrument samples photo-induced dissociation occurring during the ≈ 10 μs it takes for the ions to travel from the laser interaction region to the electrostatic analyzer.

The photo-fragment yield Γ is presumed to follow Poisson statistics,

$$\Gamma = AP^N e^{-\alpha P}, \tag{1}$$

where A is an overall scaling factor, P is the laser pulse energy, N is the number of photons required to induce the process, and α accounts for saturation of the process. The laser pulse energy P was varied using neutral density filters. Action spectra were recorded in the unsaturated regime where

$$\Gamma(\lambda) \propto \left[\sigma(\lambda)\frac{P(\lambda)}{\varepsilon(\lambda)}\right]^N, \tag{2}$$

where σ is the absorption cross section as a function of excitation wavelength λ and $\varepsilon(\lambda) = hc/\lambda$ is the photon energy. Once the value of N for a given dissociation channel is determined, this relation provides $\sigma(\lambda)$ from the experimental action spectrum $\Gamma(\lambda)$, correcting for the variation in laser output $P(\lambda)$ (measured separately) across the spectral range of interest.

B. Collision-induced dissociation

Collision-Induced Dissociation (CID) mass spectrometry measurements were performed using the EISLAB accelerator mass spectrometer at Stockholm University.[60,61] FMN anions were produced through electrospray ionization of a solution of FMN sodium salt in methanol. After mass selection by a quadrupole mass filter, a continuous beam of $[FMN–H]^-$ was accelerated to 14 keV and passed through a collision cell containing He gas (center-of-mass energy is 120 eV). The pressure in the gas cell (5×10^{-4} mbar) was fixed such that the ion beam intensity was reduced by less than 20%, ensuring that single-collision conditions dominate. Calculations have shown that such collisions deposit a broad range of excitation energies, mainly through nuclear stopping, with a mean value of ≈7 eV.[62] Fragment ions were separated using an electrostatic energy analyzer and counted with a micro-channel plate detector. As with the SepI instrument, the EISLAB instrument samples dissociation occurring within ≈10 μs after activation.

C. Dissociation energy calculations

Dissociation energies E_d for the fragmentation channels observed in this work were computed at the ωB97X-D/aug-cc-pVDZ level of theory using the Gaussian 16.B01 computational chemistry package.[63–65] The calculated dissociation energies are asymptotic (adiabatic) limits that include zero-point energy corrections. Calculated E_d values do not take into account any barriers required for intramolecular rearrangements.

III. RESULTS AND DISCUSSION

A. Mass spectra

Fragment ion mass spectra for $[FMN–H]^-$ with photo- and collision-induced activation are shown in Fig. 2. Panels (a) and (b) are photo-induced dissociation mass spectra using 450 nm light, which is a wavelength that is near the $S_1 \leftarrow S_0$ absorption band maximum for flavins in solution.[66] PID mass spectra obtained at 350 nm (not shown), corresponding to the $S_2 \leftarrow S_0$ absorption band maximum, were very similar. In panel (a), the laser pulse energy was attenuated to ≈4 mJ/pulse using a neutral density filter. At this pulse energy, single-photon events are most probable (see below for power-dependence measurements). In panel (b), the full laser power (≈14 mJ/pulse) promotes multi-photon dissociations. Panel (c) is a CID measurement recorded using EISLAB under

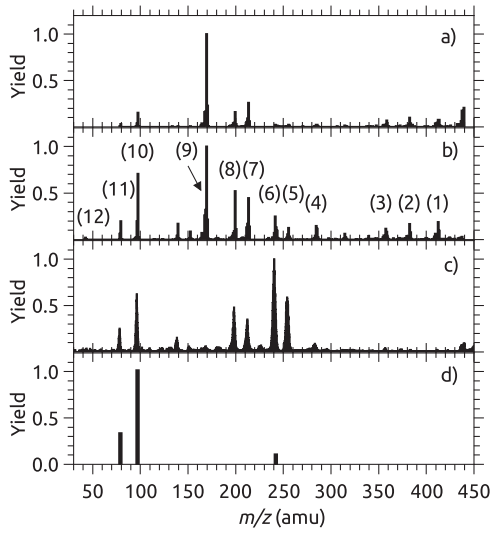

FIG. 2. Fragment ion mass spectra from $[FMN–H]^-$ following activation by (a) single-photon absorption (≈4 mJ/pulse), (b) multi-photon absorption (≈14 mJ/pulse), (c) high-energy collisions (120 eV center-of-mass energy), and (d) low-energy collisions (multiple few-eV collisions in ion trap). Photo-activation used 450 nm light (2.76 eV per photon). Peak labels in (b) refer to fragment ions identified in Table I.

single-collision conditions, which produces statistical fragmentation. Panel (d) is a low-energy CID measurement retrieved from the Massbank database[67] recorded using a commercial quadrupole/time-of-flight mass spectrometer (record number PR100554). This type of activation, in which the ions gradually build up internal energy through numerous lower-energy collisions in an ion trap, tends to promote fragmentation channels with low dissociation energies. The main fragment ions, values of N, proposed ion/fragment assignments, and calculated E_d are listed in Table I.

The single-photon PID mass spectrum [Fig. 2 panel (a)] is dominated by fragment ion **9** at m/z = 169, which comprises more than half the total fragment ion yield. Remarkably, this product is almost absent from the CID mass spectra in panels (c) and (d). Relative to ion **10** (m/z = 97, $H_2PO_4^-$), which is the dominant product in the low-energy CID spectrum and one of the lowest-energy of the observed dissociation channels (E_d = 0.81 eV), ion **9** is ~50-fold more abundant in the single-photon PID spectrum than in the statistical fragmentation pattern in panel (c). This suggests that ion **9** is the result of a non-statistical photochemical process, possibly facilitated by a mechanism involving an electronically excited state. Several other minor product ions, particularly **1** and **2**, are also significantly over-represented in the PID mass spectra relative to CID, in agreement with the results of Guyon *et al.*[52] An important caveat here is that the PID experiments deposit a known, fixed energy, whereas CID activation results in a broad distribution of internal energies.

The m/z for fragment ion **9** is consistent with the loss of formylmethylflavin ($FMFH_2$, see Fig. 1)- sometimes called formyllumiflavin. This is a well-known photo-product from FMN in basic solution.[22] Guyon *et al.* also observed positively charged $[FMFH + H]^+$ and $[FMFH_2 + H]^+$ in their experiments, which they proposed to form through a complex photoreduction/photodealkylation mechanism.[52] The present results confirm that the formation of formylmethylflavin can occur in an intramolecular process without support from a solvent or substrate. Furthermore, we find that the structure with the lowest E_d for the m/z corresponding to ion **4** is the deprotonated $FMFH_2$ species shown in Fig. 1.

TABLE I. Main fragment ions in the PID mass spectrum of $[FMN–H]^-$, precursor m/z = 455. Curly braces indicate the loss of the enclosed neutral fragment; otherwise, the fragment ion is given. N is the number of absorbed 450 nm (2.75 eV) photons required to induce the process. E_d are calculated dissociation limits relative to the phosphate deprotomer and do not account for barriers in rearrangement/dissociation processes.

Fragment	m/z	Assignment	N	E_d (eV)
1	412	{HNCO}	1	2.81
2	382	$\{(CHOH)_2CH\}$	1	…[b]
3	357	$\{H_3PO_4\}$	1	2.09
4	285	$[FMFH_2]^-$	2	2.22
5	255	$[LF–H]^-$	3	2.43
6	241	$[LC–H]^-$	3	0.74
7	213	{LC}	1	0.35
8	199	{LF}	1[a]	1.38
9	169	$\{FMFH_2\}$	1	1.45
10	97	$H_2PO_4^-$	2	0.81
11	79	PO_3^-	2	2.12
12	42	OCN^-	3	4.02

[a]The yield of 8 includes contributions from both N = 1 and 2-photon absorptions.
[b]Ion 2 could not be readily identified, and no E_d was calculated.

Other notable fragments in the single-photon PID spectrum include the loss of isocyanic acid (**1**, a well-known photofragment of uracil and thymine[68]), phosphoric acid (**3**), lumichrome (LC, **7**), and lumiflavin (LF, **8**); see structures for LC and LF in Fig. 1. LC loss was previously found to be the dominant photochemical product of flavin adenine dinucleotide mono-anions.[48] Loss of formylmethylflavin from $[FAD–H]^-$ was also observed in those experiments, but with a yield of about 30% that of LC. For $[FMN–H]^-$, this branching ratio is reversed. It is thus clear that the (phospho)ribityl sidechain has a determinative influence on the photochemistry of flavins.

Fragment ion **2** at m/z = 382 (also observed by Guyon *et al.*[52]) is not readily identified with any simple bond cleavage. Ion **2** could be due to a complex breakup of the isoalloxazine rings, e.g., HNCO + CO + H_2 or HNCO + H_2CO. This is hard to reconcile with the low activation energy implied by the 1-photon dependence and the absence of related pathways like HNCO + CO, which has been observed for smaller flavin anions.[45] Another possibility is the elimination of a part of the ribityl sidechain while retaining the phosphate group.

Our earlier PISA study on $[FMN–H]^-$ used an isomer-selection strategy to study just the phosphate deprotomer and found photoisomerization to another deprotomer with no evidence for photodissociation, including at 450 nm.[47] In those experiments, the buffer gas pressure leads to energy quenching collisions every few nanoseconds. Thus, the single-photon-induced fragmentation of

$[FMN–H]^-$ observed in the present experiments, assuming it originates from the phosphate deprotomer, is likely not from a process in the singlet excited state, since this should occur on a sub-nanosecond timescale, which would have been observed in the PISA study. It is worth outlining that the model of excited state dissociations that occur very rapidly and ground state dissociations that occur more slowly after complete statistical randomization of internal energy represent two limiting cases – there may also be quasi-statistical dissociation in which internal energy does not undergo complete statistical randomization before dissociation. For example, quantum chemical calculations on the iso-alloxazine unit *in vacuo* have found efficient intersystem crossing between the lowest excited singlet state S_1 and a triplet state.[69] In solution, this channel is deactivated by a large blue-shift of the triplet transition. In the present experiments, which in contrast to the earlier PISA study are conducted under ultra-high vacuum conditions, the triplet state may be long-lived enough to allow excited (triplet) state dissociation, promoted by statistical distribution of the singlet–triplet splitting energy. On the other hand, if the present SepI experiments involved the phosphate and the ring deprotomers (and potentially others), the observed photofragmentation pattern would be complicated with contributions from more than one deprotomer.

A PID mass spectrum for $[FMN–H]^- \cdot \mathbf{Z}$ complexes, where **Z** is the betaine zwitterion, is shown in Fig. 3. While dissociation of the complex ($[FMN–H]^- \cdot \mathbf{Z} \rightarrow [FMN–H]^- + \mathbf{Z}$) is the predominant channel, several minor ions are observed in the mass spectrum. Some of these fragments are consistent with the expected m/z for complexes of betaine with fragments of $[FMN–H]^-$. Given the mass resolution of the instrument at ≈100, it is difficult to unequivocally assign the ions at m/z = 214 and 286, which lie close to the m/z for ions **7** and **10**·**Z** or **4** and **9**·**Z**, respectively. However, the ions at m/z = 330 and 529 do not correspond to any fragments in the $[FMN–H]^-$ PID mass spectrum (Fig. 2), allowing confident assignment to **7**·**Z** and **1**·**Z**, respectively. Because the binding energy of the complex is much lower than the dissociation energies (the complex is non-covalent), the observation of zwitterion-tagged fragments suggests that fragmentation is non-statistical. The product ions **9** and **10** are also observed, which are most likely due to multi-photon processes.

In summary, the photofragmentation of isolated $[FMN–H]^-$ appears to have substantial non-statistical contributions.

B. Laser power dependence

The laser power dependencies for fragments **9**, **10**, and **6**, which are dominant fragmentation channels following the absorption of N = 1, 2, and 3 photons, are plotted in Fig. 4. The solid lines in the plot are least-squares fits to Eq. (1), holding N fixed. The plotted data have been normalized such that A = 1. The best fitting integer value of N for each fragment ion is given in Table I. Power dependence plots for other photofragments are given in the supplementary material. Many fragments, including **9**, exhibit saturation at high laser powers.

The yield of ion **8** (m/z = 199, loss of LF, see the supplementary material) is not well-represented by Eq. (1) and appears to be a combination of single- and multiple-photon processes. This could be due to two different pathways that lead to the loss of LF, or possibly due to contamination by $[LC–HNCO]^-$ (m/z = 198).

In general, there is no correspondence between the values of N determined from the power dependence measurements and the calculated dissociation energies in Table I. For example, HNCO-loss (ion **1**) has a calculated E_d = 2.81 eV, but is formed by the absorption of a single 2.75 eV photon. While the room-temperature precursor ions have significant internal energy prior to excitation, it is surprising that such a high-energy fragment is formed within the microsecond timescale sampled by the mass spectrometer. Meanwhile, several channels with lower E_d values require multiple photon absorption.

The phosphate-based fragments **10** and **11** (m/z = 97 and 79) are each formed following the absorption of two photons. These ions dominate the low-energy CID spectrum [Fig. 2(d)], indicating that they represent the lowest-energy dissociation channels or have the highest propensity for statistical dissociation. The large array of fragment ions produced following the absorption of a

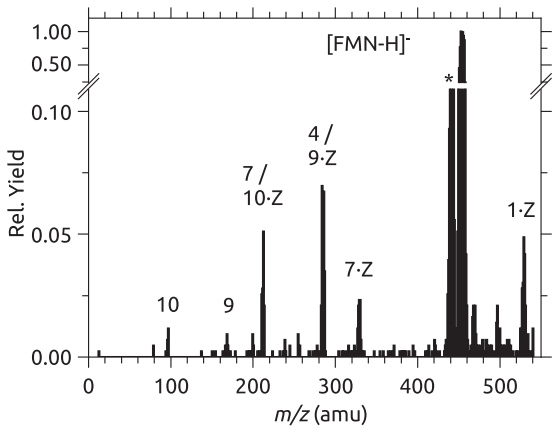

FIG. 3. PID mass spectrum of $[FMN–H]^- \cdot \mathbf{Z}$ complexes using 450 nm light. See Table I for fragment numbering. The feature marked * on the side of the dominant $[FMN–H]^-$ peak is an artifact. Note the break in the vertical axis.

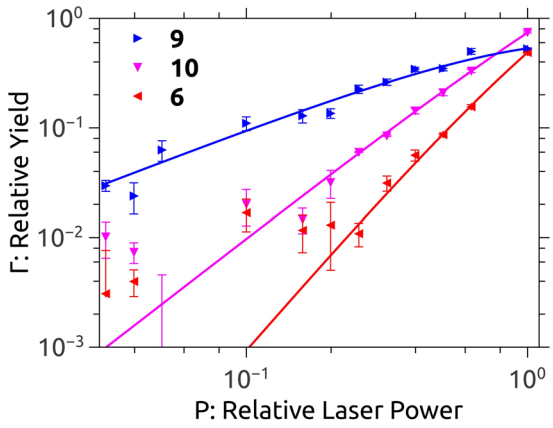

FIG. 4. Laser power dependence measurements for the most prominent fragmentation channels of $[FMN–H]^-$ induced by the absorption of 1 (**9**), 2 (**10**), or 3 (**6**) photons at 450 nm (2.75 eV). The maximum laser power (P = 1) corresponds to a pulse energy of ≈14 mJ. Note the double logarithmic scale.

single photon strongly suggests significant kinetic competition between the fragmentation channels, lending support to the non-statistical interpretation.

With the exception of ion **2** (m/z = 382), each of the observed single-photon channels has a complementary channel with a higher photon dependence. In each case, the single-photon channel is the loss of a neutral fragment, while the channel with higher photon dependence is the same fragment with one proton removed. This is likely a consequence of the photoisomerization processes identified in our earlier PISA spectroscopy study,[47] where a precursor phosphate deprotonated anion may either photoisomerize to another deprotomer or recover the ground electronic state of the phosphate deprotomer.

C. Action spectra

PID action spectra for $[FMN–H]^-$ are presented in Fig. 5. Panel (a) shows the wavelength-dependent yield of fragment ion **9**, the loss of a fragment with m/z consistent with $FMFH_2$, and the dominant fragmentation channel following absorption of a single photon. The spectra for ions **10** (black) and **6** (red), the most prominent 2- and 3-photon channels, are shown in panel (b). For a given absorbed photon number N, the action spectra for the remaining channels in Table I closely resemble the above three representative action spectra, with an average coefficient of determination of R^2 = 0.97. Panel (c) shows the photodissociation spectrum for the $[FMN–H]^- \cdot \mathbf{Z}$ complex.

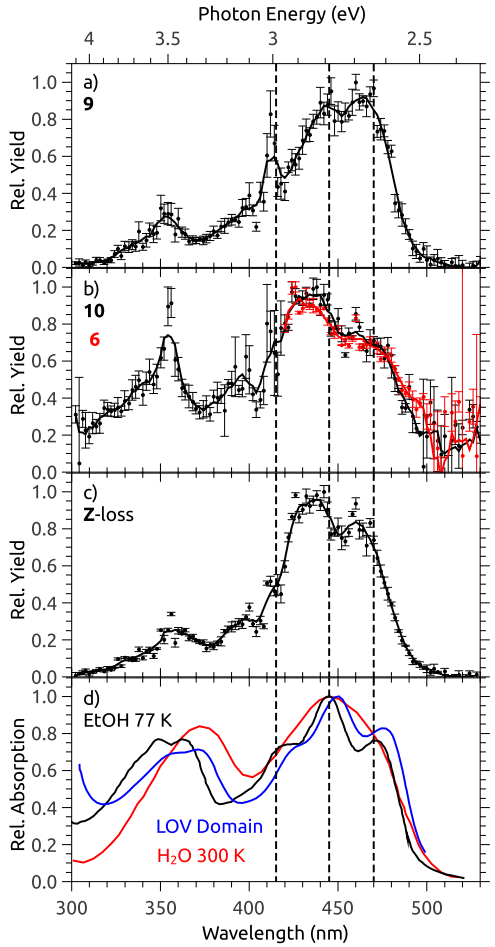

FIG. 5. PID action spectra for $[FMN–H]^-$ monitoring yield of (a) ion **9**, (b) ion **10** (black) and ion **6** (red), and (c) dissociation of $[FMN–H]^- \cdot \mathbf{Z}$ complex. The solid lines in each plot are five-point moving averages. (d) Absorption spectrum for riboflavin in ethanol at 77 K,[66] FMN in LOV domains[70] and in water.[71] Dashed vertical lines at 414, 445, and 470 nm are guide to the eye.

The spectra in Fig. 5 cover the $S_1 \leftarrow S_0$ (380–520 nm) and $S_2 \leftarrow S_0$ (300–380 nm) transitions of the flavin chromophore. The four action spectra in Fig. 5 all have a maximum response at 440 ±5 nm and a shoulder feature at 470 ±5 nm. These wavelengths are similar to the maxima in the absorption spectrum of riboflavin measured in ethanol at 77 K[66] [Fig. 5(d), black curve]. An additional maximum feature at ≈415 nm is not fully resolved in all spectra. The three-peaked structure of the $S_1 \leftarrow S_0$ band is also observed for FMN bound in Light-Oxygen-Voltage (LOV) domains of phototropin proteins[70] [Fig. 5(d), blue curve] and is due to contributions from a large number of vibronic transitions involving stretching modes of the iso-alloxazine ring system.[72,73] The protein spectrum is somewhat red-shifted, perhaps due to electric field effects.[56] The absorption spectrum of FMN in room-temperature water[71] [Fig. 5(d), red curve] is broadened and unstructured, which is typical for free flavins in solution.[72] The $S_2 \leftarrow S_0$ transition is strongly red-shifted in water due to the significant charge-transfer character of the transition.[36,69,74,75] Overall, these spectra are consistent with our previous findings that the action spectra of gaseous flavin ions deprotonated on a phosphate group closely resemble the absorption spectra of oxidized flavins in solution[36,47,48] and may more closely reproduce the spectra of flavins in protein environments.

The band maxima in the one-photon action spectrum in panel (a) are very slightly blue-shifted relative to the 77 K absorption spectrum in panel (d). The two-and three-photon spectra in panel (b) are more blue-shifted but have band profiles that more closely resemble the 77 K absorption spectrum. One factor that may have some bearing on these differences is how energy is dissipated in different environments. In particular, in condensed phases, vibrational excitation is rapidly quenched by solvent molecules. In contrast, in the gas phase, this excess excitation is not quenched and may decrease the excited state lifetime. Another factor might be fast photoisomerization and absorption of the second photon by a second deprotomer with a shifted absorption spectrum. For example, our earlier PISA spectroscopy study showed that the action spectrum for the PO4, N-3 deprotomer of FAD or the ring deprotomer of riboflavin was red-shifted compared with the PO4, PO4 deprotomer of FAD or phosphate deprotomer of $[FMN–H]^-$.[47] Here, if the first photon caused photoisomerization (which was observed for $[FMN–H]^-$ in our PISA study), then the multi-photon action spectrum would be some convolution of action spectra for the deprotomers. Whatever may be the case, caution should be exercised when interpreting subtle differences between PID action spectra, particularly those arising from the absorption of different numbers of photons.[76] The differences between the positions and relative intensities of the band maxima in the spectra in Fig. 5 may not be significant.

Complexation of $[FMN–H]^-$ with betaine does not significantly affect the position of the band maxima, as shown in Fig. 5(c).

This is consistent with the expectation that the betaine coordinates to the deprotonated phosphate group and does not perturb the electronic structure of the flavin chromophore. When the betaine is coordinated to the chromophore, a blue-shift of the $S_2 \leftarrow S_0$ spectral band would be expected toward the position in the spectrum of FMN in water [Fig. 5(d)].

One apparent difference between the gas-phase PID spectra for $[FMN–H]^-$ and the condensed-phase absorption spectra for FMN is the reduced intensity of the $S_2 \leftarrow S_0$ band (380–300 nm) relative to the $S_1 \leftarrow S_0$ band (520–380 nm). Note that two different laser systems were used for excitation in the 304–420 nm and 420–530 nm regimes, complicating a quantitative comparison of the relative intensities of these bands. A plausible explanation for the apparent suppression of the $S_2 \leftarrow S_0$ band of FMN is due to the competition between fragmentation and electron detachment or another unobserved channel. However, the adiabatic detachment energy for FMN anions deprotonated on the phosphate group has been calculated to be > 4 eV,[47] comparable to that of other phosphate anions[77] and somewhat above the $S_2 \leftarrow S_0$ transition energy. Furthermore, the PID yield for dissociation of $[FMN–H]^- \cdot \mathbf{Z}$ complexes upon $S_2 \leftarrow S_0$ excitation is also suppressed, as shown in Fig. 5(c). The electron detachment energy should be increased roughly by the binding energy of the betaine, i.e., to > 5 eV, which would clearly not be competitive with the dissociation of the complex. Given that **Z**-loss dominates the PID mass spectrum for both transitions, this also rules out the possibility that the suppression is due to competition with other unobserved fragmentation channels. Non-destructive relaxation by fluorescence would be expected to suppress the fragment yield upon $S_1 \leftarrow S_0$ excitation relative to $S_2 \leftarrow S_0$, the reverse of the observed situation. The absence of the solvent to dissipate the excess energy leads to more rapid internal conversion upon $S_2 \leftarrow S_0$ excitation and thus a reduced fluorescence quantum yield.[78] Furthermore, fluorescence has not been detected for gas-phase FMN anions despite their high quantum yield in solution,[36] perhaps due to intersystem crossing.[69] We conclude that the intrinsic transition strength is, indeed, lower in the gas phase compared to solution, perhaps due to unscreened interactions between the charged phosphoribityl sidechain and the orbitals involved in the $S_2 \leftarrow S_0$ transition, which has a significant charge-transfer character.

The $S_2 \leftarrow S_0$ transition does not appear as suppressed in the two-photon action spectrum yielding fragment ion **10** in panel (b). As discussed above, the optical spectrum upon absorption of the second photon may be significantly different from that for the first photon, especially if rapid photo-isomerization occurs after absorption of the first photon.

IV. CONCLUSION

The photo-induced dissociation of $[FMN–H]^-$ has been investigated using mass spectrometry and action spectroscopy, with the predominant photofragment possessing a mass-to-charge ratio consistent with expulsion of formylmethylflavin. The photofragment is shown to be produced through the absorption of a single photon but is not observed in low- or high-energy collision-induced dissociation mass spectra. These results suggest a non-statistical fragmentation mechanism occurring prior to the complete conversion and redistribution of electronic excitation energy across the vibrational degrees of freedom. Several other non-statistical fragmentation pathways are identified offering a guide to challenging molecular dynamics simulations. Only at higher laser pulse energies, where sequential absorption of multiple photons becomes more probable, do the fragmentation channels with the lowest dissociation energies become competitive.

The PID action spectra closely resemble the absorption by neutral, oxidized flavins. This confirms that deprotonation occurs primarily on the phosphate group with minimal perturbation to the electronic structure of the isoalloxazine chromophore. Relative to the absorption of flavins in condensed phases and to the action spectra of gas-phase flavin adenine dinucleotide mono-anions, the $S_2 \leftarrow S_0$ action spectrum band for $[FMN–H]^-$ appears to be suppressed. Having ruled out several potential explanations for this effect, we suggest that it is due to the influence of the deprotonated phosphate group. High-level calculations are needed to confirm this effect, which could have important implications for the absorption by flavins bound in proteins with high electric field strengths.

Measurements on complexes of $[FMN–H]^- \cdot$ with betaine broadly support the non-statistical conclusions drawn for bare $[FMN–H]^-$ ions through observing photofragments with betaine tags still attached. The action spectrum is very similar to that for the bare ions, suggesting that betaine binds to the phosphate group and has little interaction with the isoalloxazine chromophore.

SUPPLEMENTARY MATERIAL

The laser power dependence curves for all fragment ions in Table I are included in the supplementary material.

ACKNOWLEDGMENTS

This article is based upon work from COST Action CA18212—Molecular Dynamics in the GAS phase (MD-GAS), supported by COST (European Cooperation in Science and Technology). M.H.S. acknowledges support from the Swedish Research Council (Grant No. 2016-03675) and the Olle Engkvist Foundation (Grant No. 200-575). M.H.S. and J.N.B. acknowledge support from the Swedish Foundation for International Collaboration in Research and Higher Education (Grant No. PT2017-7328). Electronic structure calculations were carried out on the High Performance Computing Cluster supported by the Research and Specialist Computing Support service at the University of East Anglia. S.B.N. acknowledges generous support from the Independent Research Fund Denmark—Natural Sciences (Grant No. 9040-00041B).

DATA AVAILABILITY

The data that support the findings of this study are available from the corresponding author upon reasonable request.

REFERENCES

[1] V. Massey, Biochem. Soc. Trans. **28**, 283 (2000).
[2] S. O. Mansoorabadi, C. J. Thibodeaux, and H.-w. Liu, J. Org. Chem. **72**, 6329 (2007).
[3] D. Leys and N. S. Scrutton, Curr. Opin. Plant Biol. **41**, 19 (2016).

[4]I. Chaves, R. Pokorny, M. Byrdin, N. Hoang, T. Ritz, K. Brettel, L.-O. Essen, G. T. J. van der Horst, A. Batschauer, and M. Ahmad, Annu. Rev. Plant Biol. **62**, 335 (2011).
[5]I. A. Solov'yov, T. Domratcheva, A. R. M. Shahi, and K. Schulten, J. Am. Chem. Soc. **134**, 18046 (2012).
[6]R. Wiltschko, D. Gehring, S. Denzau, C. Nießner, and W. Wiltschko, J. Exp. Biol. **217**, 4225 (2014).
[7]Y.-T. Kao, C. Saxena, T.-F. He, L. Guo, L. Wang, A. Sancar, and D. Zhong, J. Am. Chem. Soc. **130**, 13132 (2008).
[8]A. Udvarhelyi, M. Olivucci, and T. Domratcheva, J. Chem. Theory Comput. **11**, 3878 (2015).
[9]A. Hense, E. Herman, S. Oldemeyer, and T. Kottke, J. Biol. Chem. **290**, 1743 (2015).
[10]B. Liu, H. Liu, D. Zhong, and C. Lin, Curr. Opin. Plant Biol. **13**, 578 (2010).
[11]J. Baier, T. Maisch, M. Maier, E. Engel, M. Landthaler, and W. Bäumler, Biophys. J. **91**, 1452 (2006).
[12]M. Orlowska, T. Koutchma, M. Grapperhaus, J. Gallagher, R. Schaefer, and C. Defelice, Food Bioprocess Technol. **6**, 1580 (2013).
[13]R. Huang, H. J. Kim, and D. B. Min, J. Agric. Food Chem. **54**, 2359 (2006).
[14]K. Huvaere, M. L. Andersen, M. Storme, J. Van Bocxlaer, L. H. Skibsted, and D. De Keukeleire, Photochem. Photobiol. Sci. **5**, 961 (2006).
[15]B. Holmström and G. Oster, J. Am. Chem. Soc. **83**, 1867 (1961).
[16]W. M. Moore, J. T. Spence, F. A. Raymond, and S. D. Colson, J. Am. Chem. Soc. **85**, 3367 (1963).
[17]E. C. Smith and D. E. Metzler, J. Am. Chem. Soc. **85**, 3285 (1963).
[18]P.-S. Song, E. C. Smith, and D. E. Metzler, J. Am. Chem. Soc. **87**, 4181 (1965).
[19]W. L. Cairns and D. E. Metzler, J. Am. Chem. Soc. **93**, 2772 (1971).
[20]P. F. Heelis, Chem. Soc. Rev. **11**, 15 (1982).
[21]I. Ahmad, Q. Fasihullah, and F. H. M. Vaid, J. Photochem. Photobiol., B **75**, 13 (2004).
[22]W. Holzer, J. Shirdel, P. Zirak, A. Penzkofer, P. Hegemann, R. Deutzmann, and E. Hochmuth, Chem. Phys. **308**, 69 (2005).
[23]I. Ahmad, Q. Fasihullah, and F. H. M. Vaid, J. Photochem. Photobiol., B **82**, 21 (2006).
[24]S.-H. Song, B. Dick, and A. Penzkofer, Chem. Phys. **332**, 55 (2007).
[25]M. Wolf, H. V. Kiefer, J. Langeland, L. H. Andersen, H. Zettergren, H. T. Schmidt, H. Cederquist, and M. H. Stockett, Astrophys. J. **832**, 24 (2016).
[26]J. N. Bull, J. T. Buntine, M. S. Scholz, E. Carrascosa, L. Giacomozzi, M. H. Stockett, and E. J. Bieske, Faraday Discuss. **217**, 34 (2019).
[27]B. F. Milne, C. Kjaer, J. Houmøller, M. H. Stockett, Y. Toker, A. Rubio, and S. Brøndsted Nielsen, Angew. Chem., Int. Ed. **55**, 6248 (2016).
[28]M. H. Stockett and S. Brøndsted Nielsen, Phys. Chem. Chem. Phys. **18**, 6996 (2016).
[29]C. Kjær, M. H. Stockett, B. M. Pedersen, and S. Brøndsted Nielsen, J. Phys. Chem. B **120**, 12105 (2016).
[30]M. H. Stockett, B. M. Pedersen, and S. Brøndsted Nielsen, Angew. Chem., Int. Ed. **56**, 3490 (2017).
[31]K. Støchkel, C. N. Hansen, J. Houmøller, L. M. Nielsen, K. Anggara, M. Linares, P. Norman, F. Nogueira, O. V. Maltsev, L. Hintermann, S. Brøndsted Nielsen, P. Naumov, and B. F. Milne, J. Am. Chem. Soc. **135**, 6485 (2013).
[32]S. Brøndsted Nielsen, J. U. Andersen, J. S. Forster, P. Hvelplund, B. Liu, U. V. Pedersen, and S. Tomita, Phys. Rev. Lett. **91**, 048302 (2003).
[33]J. C. Marcum, A. Halevi, and J. M. Weber, Phys. Chem. Chem. Phys. **11**, 1740 (2009).
[34]T. Baer and W. L. Hase, *Unimolecular Reaction Dynamics: Theory and Experiments* (Oxford University Press, 1996).
[35]M. H. Stockett, H. Zettergren, L. Adoui, J. D. Alexander, U. Bērziņš, T. Chen, M. Gatchell, N. Haag, B. A. Huber, P. Hvelplund, A. Johansson, H. A. B. Johansson, K. Kulyk, S. Rosén, P. Rousseau, K. Støchkel, H. T. Schmidt, and H. Cederquist, Phys. Rev. A **89**, 032701 (2014).
[36]L. Giacomozzi, C. Kjær, J. Langeland Knudsen, L. H. Andersen, S. Brøndsted Nielsen, and M. H. Stockett, J. Chem. Phys. **148**, 214309 (2018).
[37]A. Günther, P. Nieto, D. Müller, A. Sheldrick, D. Gerlich, and O. Dopfer, J. Mol. Spectrosc. **332**, 8 (2017).
[38]A. Sheldrick, D. Müller, A. Günther, P. Nieto, and O. Dopfer, Phys. Chem. Chem. Phys. **20**, 7407 (2018).
[39]P. Nieto, D. Müller, A. Sheldrick, A. Günther, M. Miyazaki, and O. Dopfer, Phys. Chem. Chem. Phys. **20**, 22148 (2018).
[40]D. Müller, P. Nieto, M. Miyazaki, and O. Dopfer, Faraday Discuss. **217**, 256 (2019).
[41]D. Müller and O. Dopfer, J. Phys. Chem. A **125**, 3146 (2021).
[42]A. Günther, P. Nieto, G. Berden, J. Oomens, and O. Dopfer, Phys. Chem. Chem. Phys. **16**, 14161 (2014).
[43]J. Langer, A. Günther, S. Seidenbecher, G. Berden, J. Oomens, and O. Dopfer, ChemPhysChem **15**, 2550 (2014).
[44]P. Nieto, A. Günther, G. Berden, J. Oomens, and O. Dopfer, J. Phys. Chem. A **120**, 8297 (2016).
[45]E. Matthews and C. E. H. Dessent, J. Phys. Chem. Lett. **9**, 6124 (2018).
[46]E. Matthews, R. Cercola, and C. Dessent, Molecules **23**, 2036 (2018).
[47]J. N. Bull, E. Carrascosa, L. Giacomozzi, E. J. Bieske, and M. H. Stockett, Phys. Chem. Chem. Phys. **20**, 19672 (2018).
[48]M. H. Stockett, Phys. Chem. Chem. Phys. **19**, 25829 (2017).
[49]W. D. Kumler and J. J. Eiler, J. Am. Chem. Soc. **65**, 2355 (1943).
[50]P. Drössler, W. Holzer, A. Penzkofer, and P. Hegemann, Chem. Phys. **282**, 429 (2002).
[51]G. Li and K. D. Glusac, J. Phys. Chem. A **112**, 4573 (2008).
[52]L. Guyon, T. Tabarin, B. Thuillier, R. Antoine, M. Broyer, V. Boutou, J.-P. Wolf, and P. Dugourd, J. Chem. Phys. **128**, 075103 (2008).
[53]B. Bellina, J. M. Brown, J. Ujma, P. Murray, K. Giles, M. Morris, I. Compagnon, and P. E. Barran, Analyst **139**, 6348 (2014).
[54]Y. Toker, J. Langeland, E. Gruber, C. Kjær, S. Brøndsted Nielsen, L. H. Andersen, V. A. Borin, and I. Schapiro, Phys. Rev. A **98**, 043428 (2018).
[55]C. Kjær, J. M. Lisy, and S. Brøndsted Nielsen, J. Phys. Chem. A **122**, 3211 (2018).
[56]J. Langeland, C. Kjær, L. H. Andersen, and S. Brøndsted Nielsen, ChemPhysChem **19**, 1686 (2018).
[57]K. Støchkel, B. F. Milne, and S. Brøndsted Nielsen, J. Phys. Chem. A **115**, 2155 (2011).
[58]J. A. Wyer and S. Brøndsted Nielsen, Angew. Chem., Int. Ed. **51**, 10256 (2012).
[59]M. H. Stockett, L. Musbat, C. Kjær, J. Houmøller, Y. Toker, A. Rubio, B. F. Milne, and S. Brøndsted Nielsen, Phys. Chem. Chem. Phys. **17**, 25793 (2015).
[60]M. H. Stockett, M. Gatchell, T. Chen, N. de Ruette, L. Giacomozzi, M. Wolf, H. T. Schmidt, H. Zettergren, and H. Cederquist, J. Phys. Chem. Lett. **6**, 4504 (2015).
[61]N. de Ruette, M. Wolf, L. Giacomozzi, J. D. Alexander, M. Gatchell, M. H. Stockett, N. Haag, H. Zettergren, H. T. Schmidt, and H. Cederquist, Rev. Sci. Instrum. **89**, 075102 (2018).
[62]M. H. Stockett, M. Gatchell, J. D. Alexander, U. Bērziņš, T. Chen, K. Farid, A. Johansson, K. Kulyk, P. Rousseau, K. Støchkel, L. Adoui, P. Hvelplund, B. A. Huber, H. T. Schmidt, H. Zettergren, and H. Cederquist, Phys. Chem. Chem. Phys. **16**, 21980–21987 (2014).
[63]M. J. Frisch, G. W. Trucks, H. B. Schlegel, G. E. Scuseria, M. A. Robb, J. R. Cheeseman, G. Scalmani, V. Barone, B. Mennucci, G. A. Petersson, H. Nakatsuji, M. Caricato, X. Li, H. P. Hratchian, A. F. Izmaylov, J. Bloino, G. Zheng, J. L. Sonnenberg, M. Hada, M. Ehara, K. Toyota, R. Fukuda, J. Hasegawa, M. Ishida, T. Nakajima, Y. Honda, O. Kitao, H. Nakai, T. Vreven, J. A. Montgomery, Jr., J. E. Peralta, F. Ogliaro, M. Bearpark, J. J. Heyd, E. Brothers, K. N. Kudin, V. N. Staroverov, R. Kobayashi, J. Normand, K. Raghavachari, A. Rendell, J. C. Burant, S. S. Iyengar, J. Tomasi, M. Cossi, N. Rega, J. M. Millam, M. Klene, J. E. Knox, J. B. Cross, V. Bakken, C. Adamo, J. Jaramillo, R. Gomperts, R. E. Stratmann, O. Yazyev, A. J. Austin, R. Cammi, C. Pomelli, J. W. Ochterski, R. L. Martin, K. Morokuma, V. G. Zakrzewski, G. A. Voth, P. Salvador, J. J. Dannenberg, S. Dapprich, A. D. Daniels, Ö. Farkas, J. B. Foresman, J. V. Ortiz, J. Cioslowski, and D. J. Fox, Gaussian 16 Revision B.01, Gaussian, Inc., Wallingford, CT, 2016.
[64]J.-D. Chai and M. Head-Gordon, Phys. Chem. Chem. Phys. **10**, 6615 (2008).
[65]T. H. Dunning, J. Chem. Phys. **90**, 1007 (1989).
[66]M. Sun, T. A. Moore, and P.-S. Song, J. Am. Chem. Soc. **94**, 1730 (1972).

[67]H. Horai, M. Arita, S. Kanaya, Y. Nihei, T. Ikeda, K. Suwa, Y. Ojima, K. Tanaka, S. Tanaka, K. Aoshima, Y. Oda, Y. Kakazu, M. Kusano, T. Tohge, F. Matsuda, Y. Sawada, M. Y. Hirai, H. Nakanishi, K. Ikeda, N. Akimoto, T. Maoka, H. Takahashi, T. Ara, N. Sakurai, H. Suzuki, D. Shibata, S. Neumann, T. Iida, K. Tanaka, K. Funatsu, F. Matsuura, T. Soga, R. Taguchi, K. Saito, and T. Nishioka, J. Mass Spectrom. **45**, 703 (2010).
[68]H.-W. Jochims, M. Schwell, H. Baumgärtel, and S. Leach, Chem. Phys. **314**, 263 (2005).
[69]S. Salzmann, J. Tatchen, and C. M. Marian, J. Photochem. Photobiol., A **198**, 221 (2008).
[70]M. Salomon, J. M. Christie, E. Knieb, U. Lempert, and W. R. Briggs, Biochemistry **39**, 9401 (2000).
[71]S. Turunen, E. Käpylä, K. Terzaki, J. Viitanen, C. Fotakis, M. Kellomäki, and M. Farsari, Biofabrication **3**, 045002 (2011).
[72]S. Salzmann, V. Martinez-Junza, B. Zorn, S. E. Braslavsky, M. Mansurova, C. M. Marian, and W. Gärtner, J. Phys. Chem. A **113**, 9365 (2009).
[73]B. Klaumünzer, D. Kröner, and P. Saalfrank, J. Phys. Chem. B **114**, 10826 (2010).
[74]J.-y. Hasegawa, S. Bureekaew, and H. Nakatsuji, J. Photochem. Photobiol., A **189**, 205 (2007).
[75]K. Zenichowski, M. Gothe, and P. Saalfrank, J. Photochem. Photobiol., A **190**, 290 (2007).
[76]S. M. J. Wellman and R. A. Jockusch, J. Phys. Chem. A **119**, 6333 (2015).
[77]J. A. Noble, E. Marceca, C. Dedonder, I. Carvin, E. Gloaguen, and C. Jouvet, Eur. Phys. J. D **75**, 95 (2021).
[78]K. Honma, Phys. Chem. Chem. Phys. **20**, 26859 (2018).